



Investigation of the electronic properties of Magnesium Silicon Phosphide (MgSiP_2), Zinc Silicon Phosphide (ZnSiP_2) and Zinc Silicon Arsenide (ZnSiAs_2)

Omehe N. N.* and Odezuligbo I. E.

Department of Physics, Federal University Otuoke, Bayelsa State Nigeria.

Article Information

Article # 02003
Received: 16th Jan., 2021
Revision: 24th Feb., 2021.
Acceptance: 15th March, 2021
Published: 26th March, 2021

Key Words

MgSiP_2 , ZnSiP_2 , ZnSiAs_2 ,
Electronic Bandgap,
Chalcopyrites

Abstract

Magnesium Silicon Phosphide (MgSiP_2), Zinc Silicon Phosphide (ZnSiP_2), and Zinc Silicon Arsenide (ZnSiAs_2) are materials with Chalcopyrite structure whose properties have been studied using the pseudopotential method within the density functional theory (DFT) framework. The LDA+U scheme together with the projector augmented wave (PAW) were used for the electronic band structure calculations, while the norm-conserving pseudopotentials were used for the structural optimizations. The results of the investigations predicted the materials MgSiP_2 , ZnSiP_2 and ZnSiAs_2 to be semiconductors with energy band gap values of 0.91 eV, 1.43 eV and 1.48eV respectively. The total density of states and their corresponding partial density of states were also computed

*Corresponding Author: Omehe N. N., omehennamdi@yahoo.com

Introduction

Magnesium Silicon Phosphide (MgSiP_2), Zinc Silicon Phosphide (ZnSiP_2), and Zinc Silicon Arsenide (ZnSiAs_2) are members of the ternary system $\text{A}^{\text{II}}\text{B}^{\text{IV}}\text{C}^{\text{V}}_2$ of semiconductor materials that crystallize in the chalcopyrite (CKP) structure. These materials have attracted a considerable amount of attention from both theoretical and experimental researchers due to their technological applications.

Its application has been realized for high power optical frequency conversion in the near and mid-infrared regions. It has great promise for various applications in the fields of quantum electronics, spintronics and optoelectronics, visible and infrared light-emitting diodes (LEDs), infrared detectors, infrared generation and optical parametric oscillators (Kumar and Tripathy, 2014; Arab *et al.* 2012).

Experimentally, several researchers have worked on these materials; Pena-Pedraza *et al.* (2011) employed single-crystal X-ray diffraction and Raman spectroscopy technique to investigate the Crystal and phonon structure of ZnSiP_2 . Using single-crystal X-ray diffraction, they deduced that ZnSiP_2 crystallizes in a chalcopyrite-type of structure, space group $I4_2d$ with unit cell parameters $a = 5.407(9)\text{\AA}$ and $c = 10.454(2)\text{\AA}$. Martinez *et al.* (2015) adopted the Flux technique to Single Crystal Growth and Phase Stability of Photovoltaic Grade ZnSiP_2 . A flux growth technique grows ZnSiP_2 single crystals in Zn solution.

The resulting single crystals are high purity and enable the characterization of the fundamental optoelectronic properties of ZnSiP_2 . Martinez *et al.* (2018) used a carbon-free chemical vapour deposition process for the growth of both epitaxial and amorphous thin films of ZnSiP_2 -Si. From the experiment, the optical absorption of these films reveals relatively little variation with Si content, with an optical absorption onset near 1.1 eV. Post-growth crystallization of Si-rich films resulted in epitaxial alignment, as measured by X-ray diffraction and transmission electron microscopy. These films, suggesting the possibility of band gap tuning with Si content in crystalline films. Wen and Parkinson (1997) used the Chemical vapour transport method to determine the bandgap and doping level of potential solar cell material ZnSiAs_2 . The corresponding photon energy resulted in a direct energy gaps at about 2.01 and 2.23 eV. An indirect bandgap was also found at about 1.74 eV using the square root of the photon response in this energy region, and doping density at $3.8 \times 10^{17} \text{cm}^{-3}$. Barreto *et al.* (1987), experimented the Photoconductivity spectra of ternary compound ZnSiP_2 using a computer-controlled spectrometer method that allows the photoresponse to be measured for a desired amount of time at each wavelength, and a band gap of 2.05eV was reported.

Theoretically, these materials have received attention. Kocak and Ciftci (2016), analysed the structural,

electronic and optic properties of Ni doped MgSiP₂. Jaffe and Zunger (1984), investigated the Electronic structure of the ternary pnictide semiconductors ZnSiP₂, ZnGeP₂, ZnSnP₂, ZnSiAs₂, and MgSiP₂ using self-consistent all-electron density-functional electronic-structure calculations to clarify the role of the zinc 3d. Basalaev *et al.* (2005), studied the electronic structure of triple phosphides MgSiP₂, ZnSiP₂, and CdSiP₂ using pseudopotential calculations. Kocak *et al.* (2016) explored the structural and thermoelectronic properties of chalcopyrite MgSiX₂ (X = P, As, Sb) using density functional theory with five different generalized gradient approximation (GGA) functionals: Perdew–Wang, Perdew–Burke–Ernzerhof, revised Perdew–Burke–Ernzerhof, modified Perdew–Burke–Ernzerhof for solids, and Armiento–Mattson, as well as the local density approximation. They reported that these compounds are direct-bandgap semiconductors, exhibiting ductile elastic nature and anisotropic behavior of both elastic and optical properties. Arab *et al.* (2012) studied the pressure effect on the structural, elastic, and electronic properties of ZnSiP₂ by employing the plane wave pseudo-potential method (PP-PW) within the generalized gradient approximation (GGA-PW91). They found that ZnSiP₂ undergoes a structural phase transition under pressure from chalcopyrite to rocksalt type structure at 35 GPa, and analysis of the bulk modulus to shear modulus (B/G) ratio shows that ZnSiP₂ must be classified as a brittle material. The reported band gap was 1.34 eV. Bidai *et al.* (2020), worked on Carbon substitution enhanced electronic and optical properties of MgSiP₂ chalcopyrite through TB-mBJ approximation.

The calculated the optical properties and the results showed that the average absorption coefficient of MgSi_{1-x}C_xP₂ alloys is improved in the visible light region ($\alpha \sim 10^5 \text{ cm}^{-1}$). Ibrahim *et al.* (2017) did research on the structural parameters and optoelectronic properties of Mg-IV-V₂ (IV=Si, Ge, Sn and V=P, As) compounds using full-potential linearized augmented plane wave (FP-LAPW) method and reported a bandgap of 2eV for MgSiP₂. Xu *et al.* (2008) studied the structural, electronic and optical properties of the chalcopyrite semiconductor ZnSiAs₂ with Full potential linearized augmented plane wave plus local orbital method (FPLAPW+lo). They reported a direct bandgap of 1.152eV. They also noted that there is quite a strong hybridization between the

3p states of Si atom and 4p states of As atom. In this study, the LDA+U scheme will be used to investigate the electronic properties of MgSiP₂, ZnSiP₂ and ZnSiAs₂. To the best of our knowledge, this scheme not being applied to study these materials.

Computational Details

The ternary Chalcopyrites belong to the space group (space group number 122). The Chalcopyrite structure is a superlattice of the Zinc-blende structure. Silicon (Si) atoms are at the 4a site For MgSiP₂, the Magnesium (Mg) atoms are at the 4b site, while for ZnSiP₂ and ZnSiAs₂, the Zinc (Zn) atoms are at the 4b site of the Wyckoff's atomic coordinates. The Phosphorous (P) in MgSiP₂ as well as ZnSiP₂ is at the 8d site, this also applies to Arsenic (As) in ZnSiAs₂ that is at the 8d site. The number of formula unit in the unit cell (z value) for MgSiP₂, ZnSiP₂ and ZnSiAs₂ is four (4), which gives a total of 16 atomic coordinates of three (3) types. Here, structure optimization, electronic band structure, the total and partial density of states were computed for the materials under investigation. The pseudopotential method was used within the density functional theory (DFT) framework. The Abinit (Gonze *et al.*, 2002; Gonze *et al.*, 2005) a quantum suite of computer codes was used in this study. In the structural optimization of the materials, the starting lattice parameters were adopted from the experimental work of Murtaza *et al.* (2014). The x component of the atomic positions at the Wyckoff's 8d site was allowed to evolve while the others were fixed. The self-consistency iterations continued until a force tolerance of 0.01 was reached. For the energy bands, the total density of states (DOS), and partial density of states (PDOS), the LDA+U scheme was used with the projector augmented wave as implemented in the Abinit package except for MgSiP₂ where only the LDA component was used since there are no d orbital components in the configuration of its constituent atoms.. The following were states included in the computations, Mg has the 2s, 3p, 3s orbitals, Zn has 3s,3p,3d, 4s: Si has 3s and 3p: P has 3s and 3p: As has 4s and 4p. The plane waves were generated by a kinetic energy cut-off of 20 Ha, a Monkhorst-Pack shifted grid 4x4x4 yielding a mesh of 256 k-point, which was used for the Brillouin zone integration. The self-consistent computation was deemed to have achieved convergence when the energy tolerance of 10⁻⁸ was achieved.

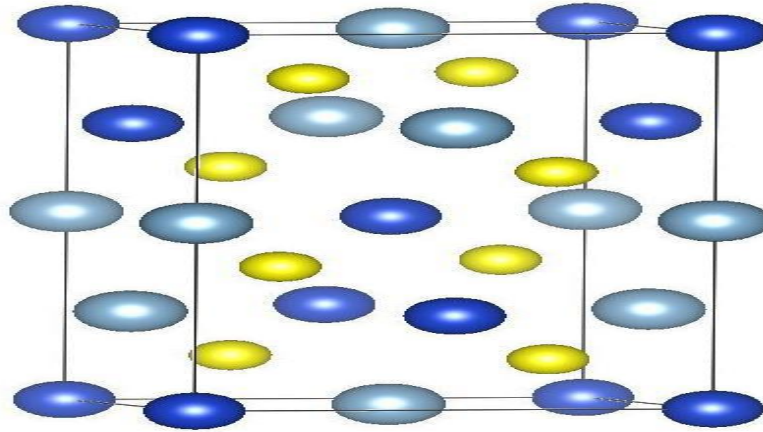


Figure 1: The structure used in the computations. Yellow balls represent P or As atoms, Blue balls for Mg atoms and Grey for Si atoms.

Table 1: Optimization results

	$a(\text{\AA})$	$c(\text{\AA})$	x	y	z
MgSiP ₂	5.7383	10.1522	0.0	0.0	0.0
			0.0	0.0	0.5
			$u=0.25$	0.25	0.125
Experiment	5.718 ^f	10.115 ^f	$u=0.292^f$		
ZnSiP ₂	5.6650	11.3310	0.0	0.0	0.0
			0.0	0.0	0.5
			$u=0.3060$	0.25	0.125
Experiment	5.612 ^a , 5.399 ^b	10.878 ^a , 10.435 ^b	0.267 ^g		
ZnSiAs ₂	5.3810	10.4013	0.0	0.0	0.0
			0.0	0.0	0.5
			$u=0.2624$	0.25	0.125
Experiment	5.612 ^c , 5.6087 ^d , 5.609 ^e	10.878 ^c , 10.8783 ^d , 10.880 ^e	0.26 ^h		

^aPena-Pedraza *et al.* (2012); ^bAbraham and Bernstein (1970); ^c Masumoto (1966); ^dFedorchenko *et al.* (2017);
^eShaukat *et al.* (1974); ^fBasalaeu *et al.* (2005); ^gKumar *et al.* (2014); ^hMurtaza *et al.* (2014)

Results and Discussion

The results of the optimizations are shown in table 1 and the structure shown in fig 1. Figures 2a 2b and 2c shows the electronic band structure of the materials under investigation, that is, MgSiP₂, ZnSiP₂ and ZnSiAs₂ respectively. The band structure is a plot of energy against high symmetry points in the first brillioun zone. The dashed lines (Point 0) are chosen to coincide with the top of the valence band. It is clear from these figures that the valence band maximum (VBM) and the conduction band minimum (CBM) both occur at the Γ point, resulting in a direct bandgap nature (Γ - Γ) in all studied materials. The band around the Fermi level are flat, this might indicate that transition from other high

symmetry points is notable. The M point of high symmetry for these materials shows a slight decrease in band energy from the Fermi level for MgSiP_2 , ZnSiP_2 , and ZnSiAs_2 . Computational results presented in fig 1 indicate that the materials MgSiP_2

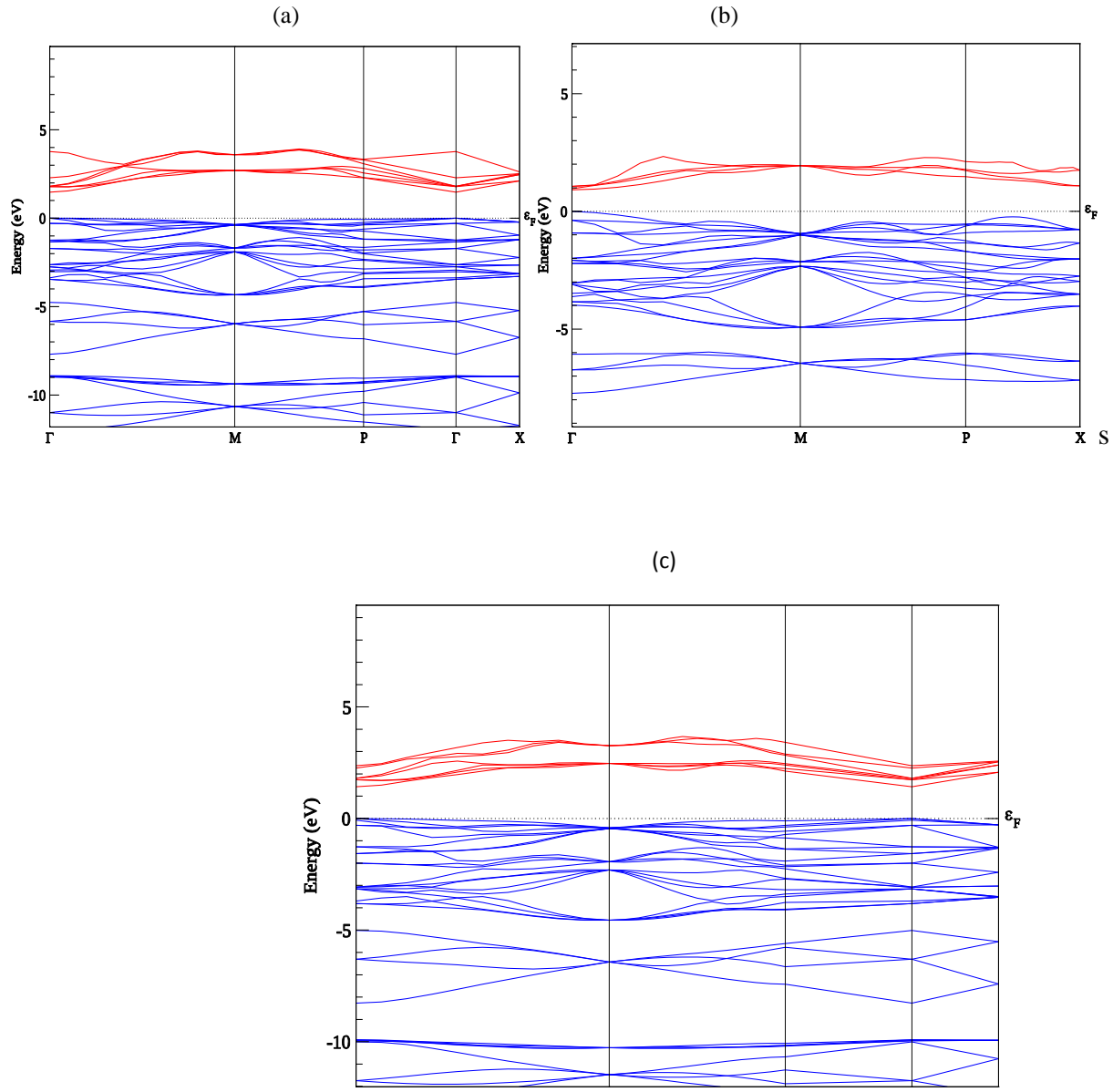


Figure 2: The electronic band structure of (a) ZnSiP_2 (b) MgSiP_2 (c) ZnSiAs_2 . E_F indicates the Fermi level.

These results are in excellent agreement with experimental and other theoretical results. The computed band gap for MgSiP_2 is 0.91 eV and the experimental bandgap as reported by Jaffe and Zunger (1984) for MgSiP_2 is 2.3 eV. Kocak *et al.* (2016) reported a theoretical value that ranges from 1.076 to 1.491, Ibrahim *et al.* (2017) reported a ranged from 1.2 – 2.0 eV, and Boukabrine *et al.* (2016) 1.985 eV. The computed bandgap for ZnSiAs_2 is 1.43 eV, and the experimental value reported in the literature by Wen and Parkinson (1997) for ZnSiAs_2 ranged from 2.01 to 2.23, Xu *et al.* (2008) and Murtaza (2014) reported a theoretical value of 1.152 eV and 1.2 eV respectively. The computed bandgap for ZnSiP_2 is 1.48 eV, and the experimental value reported in the literature by Barreto *et al.* (1987) is 2.05

eV and Martinez *et al.* (2015) 2.1eV. Arab *et al.* (2012) reported a computed value of 1.34 eV, and Kumar *et al.* (2014) reported a theoretical value of 1.38 eV.

The contribution of different states in the band structure can be studied from the density of states (DOS). The total density of states of MgSiP₂, ZnSiP₂ and ZnSiAs₂ are plotted in fig 3a to 3c respectively, and the plot is DOS versus energy in Hartree. All the features of the band structure plots are well reproduced in the TDOS graph. The bandgaps are seen at the Fermi level of the TDOS plot, re-emphasizing the semiconducting nature of these materials. The various peaks and curves in the TDOS graphs in figure 3 correspond to the different sections of the band structure (fig 2).

To clarify the contribution of each orbital of these atoms, we computed partial density of states (PDOS), that is, the orbital components to the density of states of the materials under investigation as presented in figs 4 to 6 for ZnSiP₂, ZnSiAs₂ and MgSiP₂ respectively. The orbital decomposition of the TDOS of ZnSiP₂ is presented in fig 4. The Zn-p states are dominant about -0.8 Ha and have a sharp narrow peak suggesting a less dispersion as seen from fig 4a. About the zero marks on the energy axis, it can be seen from fig 4b that the Si-p state is dominant, and also slightly in the conduction band. Figure 4c shows P-s states are dominant at about -0.4 Ha while the P-p state is predominant around the Fermi level. States also around the Fermi level are Si-s and P-p.

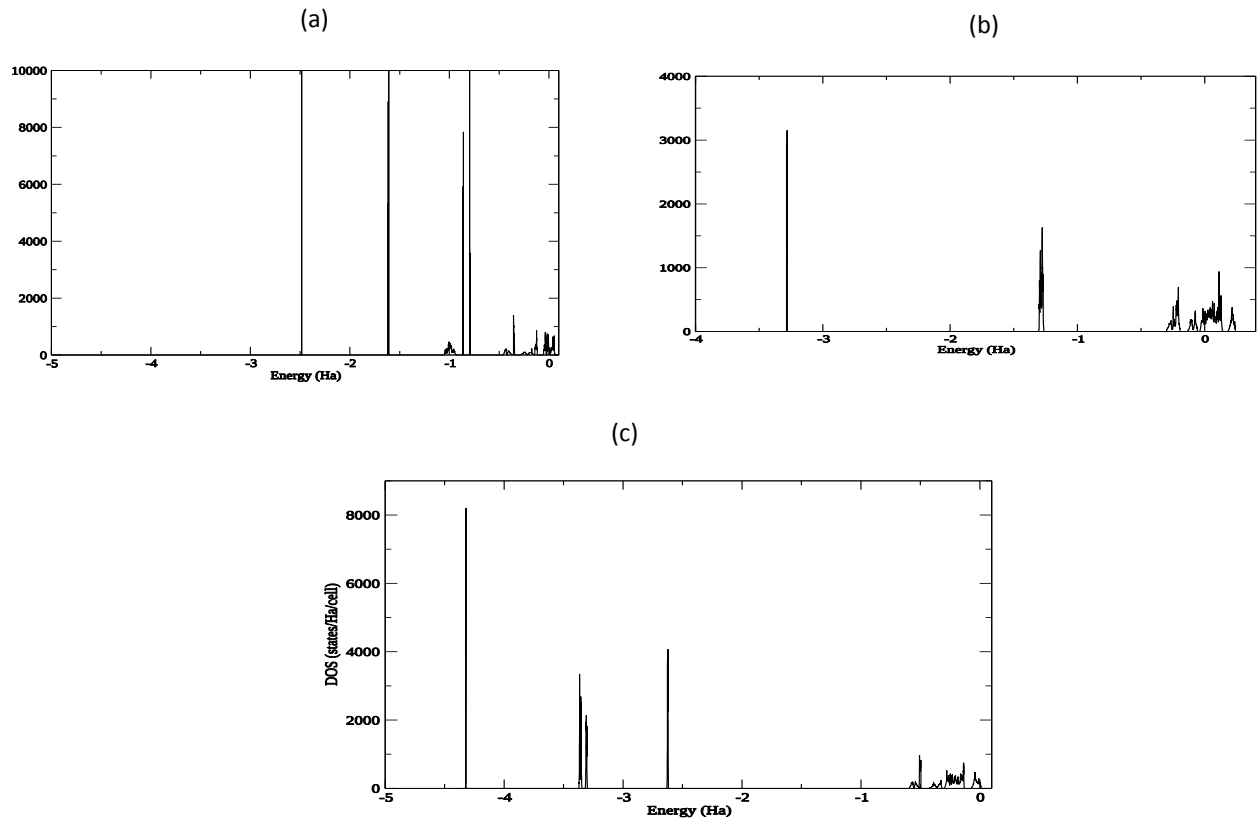


Figure 3: Total density of states for (a) ZnSiP₂ with the Fermi level at 0.0 Ha (b) MgSiP₂ with the Fermi level at 0.05 Ha (c) ZnSiAs₂ with the Fermi level at -0.05 Ha

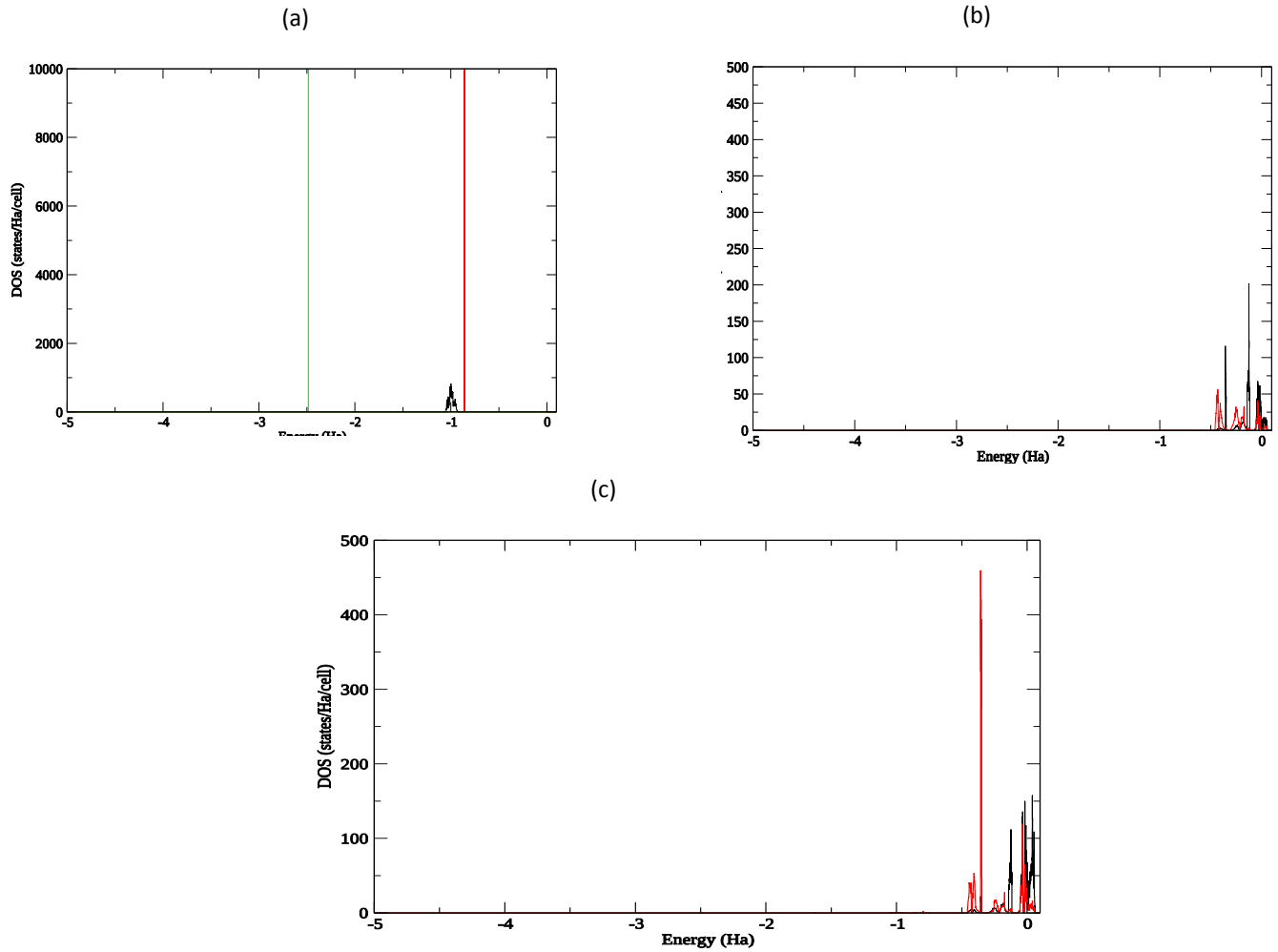
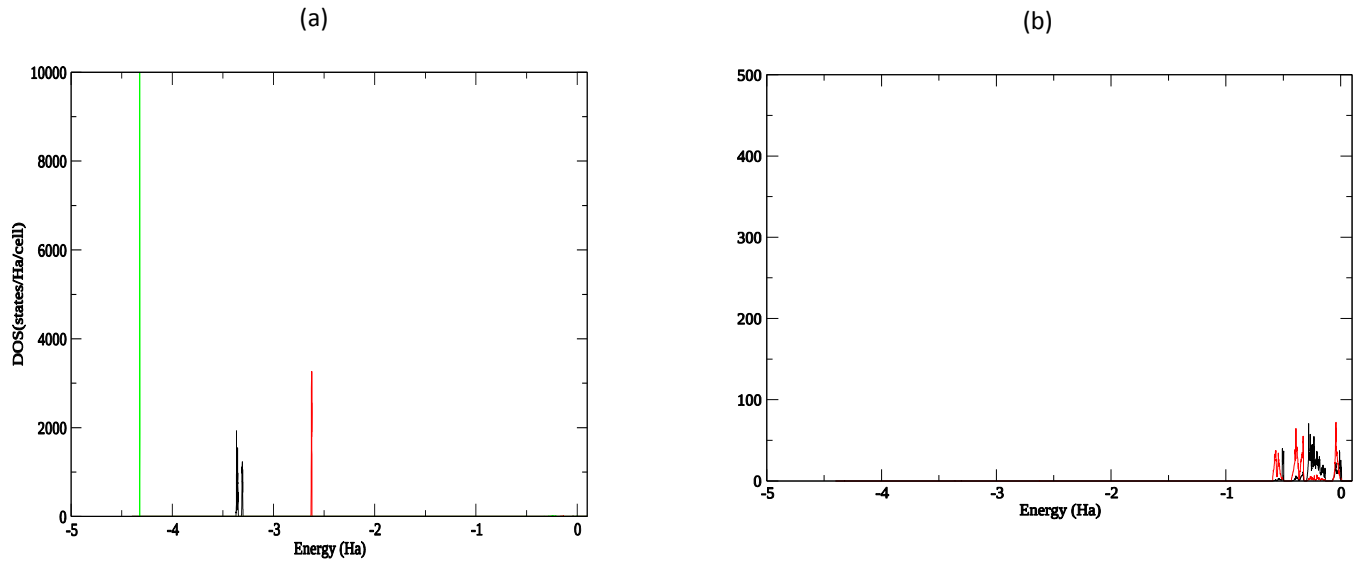


Figure 4: The partial density of states of $ZnSiP_2$. (a) orbital contributions from the Zinc Zn atom (b) orbital contributions from the Silicon Si atom (c) orbital contributions from the Phosphorous P atom



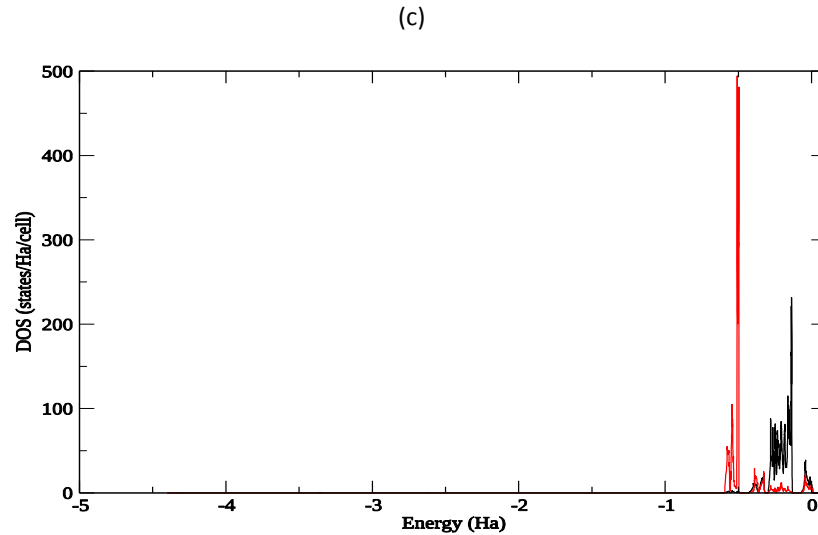
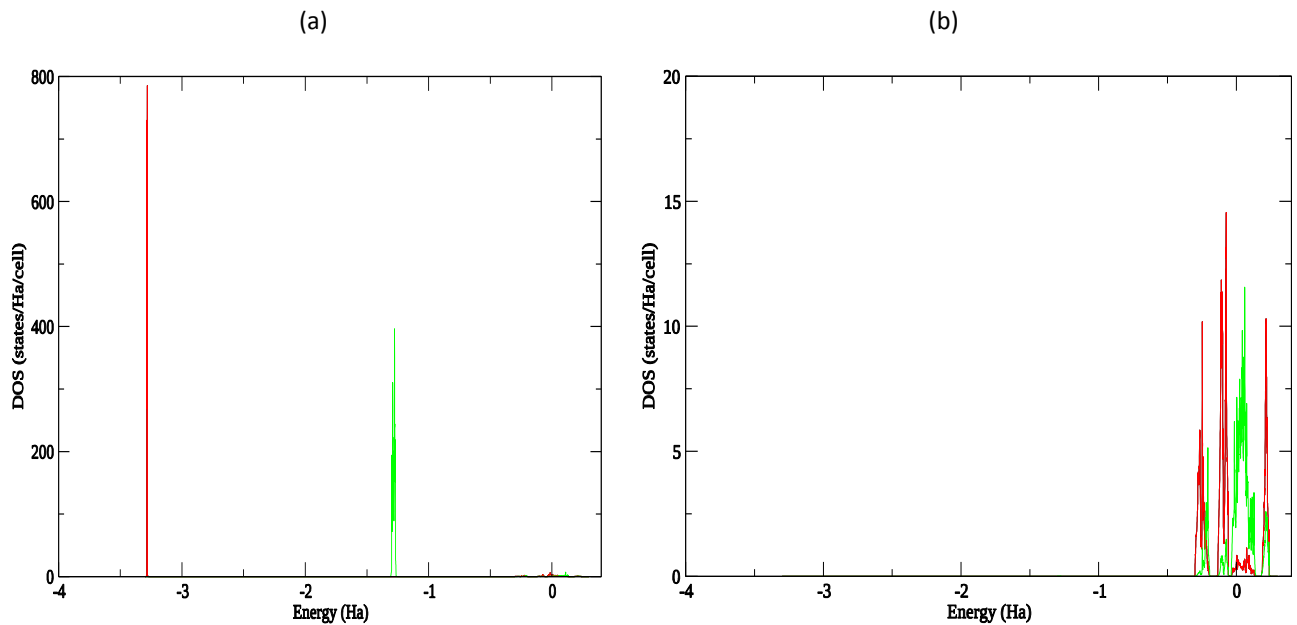


Figure 5: The partial density of states of ZnSiAs₂. (a) orbital contributions from the Zinc Zn atom (b) orbital contributions from the Silicon Si atom (c) orbital contributions from the Arsenic As atom

The orbital decomposition of the TDOS of ZnSiAs₂ is presented in fig 5. Zn-p dominates at about -2.7 Ha as shown in fig 5a. Si-s states dominate the zero mark as clearly seen in fig 5b. The zero mark is also made up of Si-p. From fig 5c, As-s states are dominant at about -0.05 Ha, and also occupies the Fermi level with As-p where it is predominant.



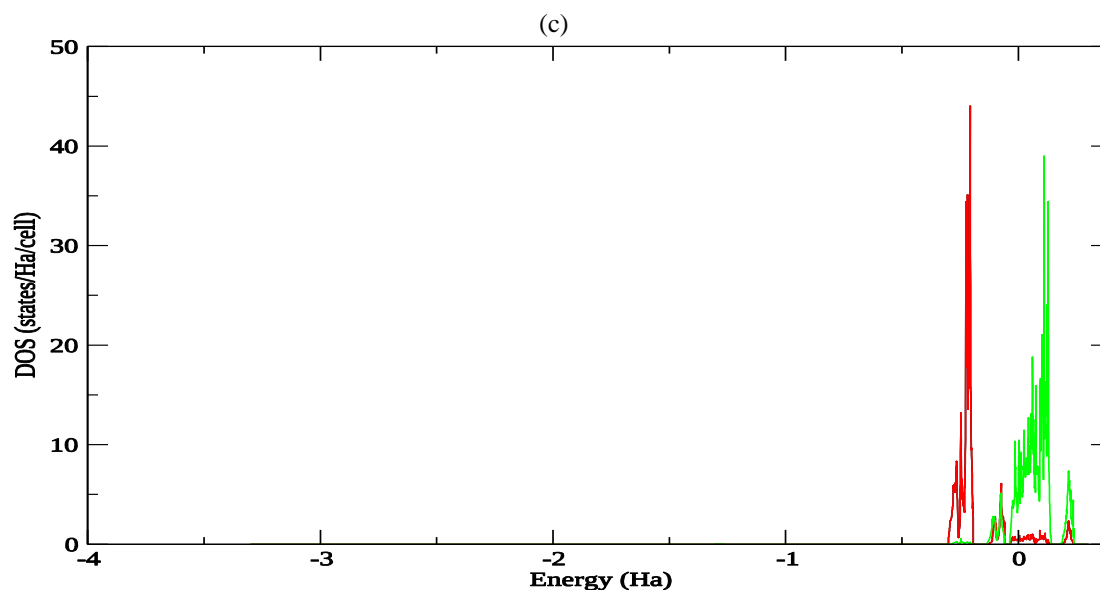


Figure 6: The partial density of states of MgSiP_2 . (a) orbital contributions from the Magnesium Mg atom (b) orbital contributions from the Silicon Si atom (c) orbital contributions from the Phosphorus P atom

The orbital decomposition of the TDOS of MgSiP_2 is presented in figure 6. The peak representing the Mg-s states is very sharp and narrow, also suggesting a far dispersion and dominates the far left as shown in figure 6a. Si-s and Si-p states cluster the zero mark where Si-s dominates as clearly seen in figure 6b. The Si-s and P-p state is the dominate state in the conduction band. The P-s state is the dominate state in the valence at about 0.03 Ha. The states at the zero mark are made up of P-s and P-p. Other states in the conduction band apart from the dominant states are the Si-p and S-s.

Conclusion

The electronic band structure, the total density of states and the partial density of states for MgSiP_2 , ZnSiP_2 and ZnSiAs_2 Chalcopyrite materials have been studied using the pseudopotential method within the density functional theory (DFT) framework. The LDA+U scheme together with the projector augmented wave (PAW) were used for the electronic band structure calculations, while the norm-conserving pseudopotentials were used for the structural optimizations. The results of the investigations predicted the materials MgSiP_2 , ZnSiP_2 and ZnSiAs_2 to be semiconductors with energy band gap value of 0.91 eV, 1.43 eV and 1.48 eV respectively. The transition points in the band structure are all notable because of the narrowness of the bands about the Fermi level. The total density of states and their corresponding partial density of states were also computed and interpreted. The Si-p and Si-s states were the dominate states in the conduction band for ZnSiP_2 and MgSiP_2 respectively, and Si-s, dominating the Fermi level for ZnSiAs_2 .

Competing interests' statement: The authors declare there are no competing interests.

Funding statement: The authors declare no specific funding for this work.

References

Abrahams, S. C. and Bernstein J. L. (1970). Crystal Structure of Luminescent ZnSiP_2 , *The Journal of Chemical Physics* 52, 5607; doi: 10.1063/1.1672831
Arab, F., Sahraoui, F. A., Haddadi, K., and Louail, L. (2012). Ab initio investigations of structural, elastic and electronic properties of ZnSiP_2 : Pressure effect. *Journal of Computational Materials Science* 65, 520–527.

Barreto, D., Luengo, J., De Vita, Y., and Joshi, N.V. (1987) Photoconductivity study of ZnSiP_2 and CdSe:Cu by a computer-controlled spectrometer. *Applied Optics* 26 (24)

Basalaev, Y. M., Gordienko, A. B., and Poplavnoi, A. S. (2005). Electronic structure of triple phosphides

MgSiP₂, ZnSiP₂, and CdSiP₂. *Russian Physics Journal*, 48(1).

Bidai, K., Tabeti, A., Mohammed, D.S., Seddik, T., Batouche, M., Özdemir, O., and Bakhti, B. (2020) Carbon substitution enhanced electronic and optical properties of MgSiP₂ chalcopyrite through TB-mBJ approximation. *Computational Condensed Matter* 24 (490)

Boukabrine, F., Chiker F., Miloua, R., Kebbab, Z., Khenata, R., Prakash, D., Omran, S., and Verma, K.D. (2016). Combined theoretical studies of the optical characteristics of II-IV-V₂ semiconductor thin films: *Optical Materials* 54, 200–206

Gonze, X., Beuken, J.M., Caracas, R., Detraux, F., Fuchs, M., Rignanese, G.M., Sindic L., Verstraete, M., Zerah, G., Jollet, F., Torrent, M., Roy, A., Mikami, M., Ghosez, P.H., Raty, J.Y. and Allan, D.C. (2002). First-principles computation of material properties: the Abinit software project, *Computational Materials Science* 25, 478-492. ([http://dx.doi.org/10.1016/S0927-0256\(02\)00325-7](http://dx.doi.org/10.1016/S0927-0256(02)00325-7)).

Gonze, X., Rignanese, G.M., Verstraete, M., Beuken, J.M., Pouillon, Y., Caracas, R., Jollet, F., Torrent, M., Zerah, G., Mikami, M., Ghosez, P.H., Veithen, M., Raty, J.Y., Olevano, V., Bruneval, F., Reining, L., Godby, R., Onida, G., Hamann, D. R. and Allan D. C. (2005). A brief Introduction to the Abinit software package. *Z. Kristallogr.* 220, 558-562.

Ibrahim, M., Ullah, H., Ullah, S. J., Ali, M., and Ashiq, G. (2008). Structural Parameters and Optoelectronic Properties of Mg-IV-V₂ (IV=Si, Ge, Sn And V=P, As) compounds. *Surface Review and Letters* 25(8), 1-11. doi: 10.1142/S0218625x18501081.

Jaffe, J. E., and Zunger, A. (1984). Electronic structure of the ternary pnictide semiconductors ZnSiP₂, ZnGeP₂, ZnSnP₂, ZnSiAs₂ and MgSiP₂. *Physical Review* 30 (2)

Kocak, K., and Oztekin C., Y. (2016). Analysis of the structural, electronic and optic properties of Ni doped MgSiP₂ semiconductor chalcopyrite compound. doi:10.1063/1.4944245.

Kocak, K., Oztekin C., Y., and Surucu, G. (2016). Structural and Thermoelectronic Properties of Chalcopyrite MgSiX₂ (X = P, As, Sb). *Journal of*

Electronic Materials, doi: 10.1007/s11664-016-4836-3

Kumar, V., Tripathy, S.K., Jha, V., and Singh, B.P. (2014) Second-harmonic generation properties of II-IV-V₂ chalcopyrite semiconductors *Physics Letters A* 378 519–523

Martinez, A.D., Oritz, B.R., Johnson, N.E., Baranowski, L.L., Krishna, L., Choi, S., Dippo, P.C, To, B., Norman, A.G., Stradins, P., Stevanovic, V., Toberer, E.S., and Tamboli A.C. (2015) Development of ZnSiP₂ for Si-Based Tandem Solar Cells *Journal of Photovoltaics* 5, (1)

Martinez, A.D., Miller, E.M., Norman, A.G., Schnepf, R.R., Leick, N., Perkins, C., Stradins, P., Toberer, E.S., and Tamboli, A.C. (2018). Growth of amorphous and epitaxial ZnSiP₂-Si alloys on Si. *Journal of Materials Chemistry*:12, (6): 12-17

Masumoto, K., Isomura, S., and Goto, F. (1996). The preparation and properties of ZnSiAs₂, ZnGeP₂, and CdGeP₂, semiconducting compounds. *J. Phys. Chem. Solids* 27, 1939-1947

Murtaza, G., Khenata, R., Reshak, A.H., Hayat, S.S. (2014) Optoelectronic properties of XYAs₂ (X=Zn, Cd; Y= Si, Sn) chalcopyrite compounds. *Journal of optoelectronics and advanced materials.* 16, 110 - 116

Pena-Pedraza, H., Lopez-Rivera, S.A., Martin, J.M., Delgado, J.M., and Power, Ch. (2012). Crystal and phonon structure of ZnSiP₂, a II-IV-V₂ semiconducting compound *Materials Science and Engineering B* 177, 1465– 1469

Shaukat, A., Burzlaff, H., Serrat, M., and Meloni, F. (1984). Experimental and theoretical charge density distribution studies in ZnSiAs₂ *Journal of Progress in crystal growth and characterization* 10, 31-36

Xu, B., Han, H., Sun, J., and Yi, L. (2009) The structural, electronic and optical properties of the chalcopyrite semiconductor ZnSiAs₂. *Physica B* 404 1326–1331

Wen, Y.C. and Parkinson, B. A. (1997) Preparation and Photoelectrochemical Characterization of ZnSiAs₂ Crystals. *J. Phys. Chem.*, 101, 2659-2662